Control the Metal Grain Boundary Recrystallization Evolution by the Laser Radiation Electric Field Strength Direction Under Cyclic Thermal Loading

Makin Vladimir Sergeevich

Additional information is available at the end of the chapter

Abstract

The spatial grating formation at metal surface under the linear polarized laser radiation action is briefly considered. The spatial grating periods are well described in framework of universal polariton model (UPM) and are well-defined physical quantities. The production of new-type gratings (quasi-gratings) at laser power densities lower than the metal melting threshold with power-dependent typical spatial scale and polarization-dependent orientation are discovered. The regularities of quasi-grating production are experimentally studied. The physical model of quasi-grating formation explaining the anisotropic character of metal recrystallization is suggested. The anisotropy is caused by the directed electron flux interaction with grain boundaries. The electron flux results from the drag effect of electrons by surface plasmon polaritons (SPPs). SPPs are excited by incident laser radiation on the surface irregularities including the grain boundaries. The volume analog of considered effect is the electroplastic one, and some of its regularities are considered.

Keywords: metal, anisotropic recrystallization, laser radiation, linear polarization, grain boundary movement, surface plasmon polaritons, electrons drag by surface plasmon polaritons, electroplastic effect

1. Introduction

It is known that the separated direction usually arises on the condensed matter surfaces and in bulk under the action of linear polarized laser radiation. The arising phenomena of linear polarized electric field strength-oriented grating formation are well described in framework

INTECH
open science | open minds

of universal polariton model (UPM) of laser-induced condensed matter damage [1]. The UPM well describes the spatial periods for normally oriented (**g** ‖ **E**) [2] and abnormally oriented (**g** ⊥ **E**) gratings (**g**) as for long pulse durations [3] as for ultrashort laser pulses [4, 5]. Here **E** is the electric field strength vector of incident laser radiation. In the later case, the effect exists for condensed media with different physical properties: metals, semiconductors, and dielectrics. So the peculiar directions arise due to the vector nature of light, surface plasmon polaritons [6] and channel (wedge) surface plasmon polariton [4] excitation, and participation in the interference process. The produced spatial gratings have some distribution in directions and periods for ultrashort pulse durations, but for long pulses depending on laser wavelength and optical properties of boundary materials, the periods have well-defined values. In our experiments with the incident laser radiation of nanosecond duration, the field-oriented grating is formed with periods defined not so strictly as the universal polariton model dictated. So, the problem is the physical mechanism of the observed effect.

The contemporary theory of condensed media describes the spatially hierarchical synergetic behavior of structures in solids, including under conditions of relaxation from nonequilibrium state [7]. One example is the metal recrystallization [8], including laser-induced recrystallization [9]. It is known that the process of collecting recrystallization on metal's surface caused by heating up to the melting point is followed by grain boundary movement and enlarging of their scales [10]. This is the isotropic process because of the lack of separated direction in considered system. There are known experiments on metal films deposited on dielectric substrate recrystallization under cyclic heating by laser radiation up to the melting point followed by lateral spatial grain-scale enlargement [9]. The grain-scale growth in average is isotropic due to the absence of separated direction in considered system *metal-dielectric-laser radiation*.

2. Results

We studied the self-organized phenomena of micro- and nanostructure formation on metal surfaces under action of series of laser radiation pulses (λ = 1064 µm, τ = 10, 100 ns) at near-normal incidence upon the mechanically polished titanium surface (VT—1-0). Formation of three types of structures versus the laser power density (q) and pulse number (N) was observed. At q values corresponding to partial metal melting during the pulse, the creation of resonant periodic grating with period

$$d_0 = \lambda \, / \, \eta \approx 1.04 \; \mu m \qquad (1)$$

and orientation $\mathbf{g_0}$ ‖ **E** written as surface relief modulation was observed. Here η is the real part of the refractive index for titanium-air boundary for surface plasmon polaritons. Their formation was due to the interference of the incident laser radiation and surface plasmon polaritons excited by it (universal polariton model (UPM) [11]).

The second type of the structures (abnormal one) was also observed in the regime of partial metal melting; it was observed predominantly on the ridges of the main resonant relief (of the first-type gratings) and had the period [5]:

$$d = \lambda / 4\xi \approx 0.21 \; \mu m \tag{2}$$

and anomalous orientation $\mathbf{g} \perp \mathbf{E}$. Their formation was caused by participation of the wedge surface plasmon polaritons (WSPPs) guided by ridges of the main resonant relief (structures of the first type) explained by the nonlinear mathematical model of spatial period formation [12]. Here ξ is the real part of the refractive index for wedge surface plasmon polaritons of the considered boundary.

The third type of structures was observed only for laser pulse duration $\tau \approx 10$ ns at q values not exceeding the material melting threshold. The produced microrelief was the quasi-grating $\mathbf{G}$, the period of which varied by laser radiation power density and orientation was $\mathbf{G} \perp \mathbf{E}$. Note that in contrast to the resonant micro- and nanostructures (of first and second types), the quasi-gratings had no precise value of the period according to formula (1) or (2). So, the third type of structures could not be explained in the framework of the universal polariton model. To explain their occurrence, the original model was developed.

As the samples in experiments the VT1-0 titanium plates mechanically polished with optical quality were used (geometrical sizes: 7 mm diameter and 1 mm thickness). The Q-switched linear polarized radiation of Nd^{3+}:Yttrium Aluminum Garnet (YAG) laser ($\lambda = 1064$ nm, $\tau = 10$ ns, 100 ns, f ≤ 12.5 Hz) with power density q ≤ 0.5 MW/cm^2 was used for sample irradiation. Laser radiation was focused by lens with focal length f = 18 cm into the typical diameter of irradiated spot (0.6 ÷ 1) mm. The sample surface reflectivity dynamics from pulse to pulse at $\lambda = 632.8$ nm was measured with the help of integrated sphere. The residual surface relief was studied by optical microscopy (preferentially in dark field) and atomic force microscopy. The main experiments were made with normal incidence of laser radiation or for p-polarized radiation and not high angles of incidence.

In experiments, the following evolution of the micro- and nanorelief was observed, which can be by convention divided by three consecutive stages. The *first stage* was the fine-scale formation of quasi-isotropic nanorelief, the typical size of which was less than the optical microscope resolution value in mode of fine-scale deformation grain boundary network. The *second stage* was the rise of mean grain-size dimension with the grain anisotropy appearance. The grain boundaries were observable with optical microscopy. This is the typical stage of collective recrystallization. At the *third stage*, the grain boundary was gradually converted into quasi-linear relief having typical size $s \sim (4 \div 6)$ μm. The relief was formed in mode of thermal grooves (see **Figure 1**). Its quasi-grating vector $\mathbf{G}$ was near perpendicular to $\mathbf{E}_t$: Here $\mathbf{E}_t$ is the tangential projection of electric field strength vector of the incident radiation. Especially note that the s value was power density dependent and rising with q. The s value also was varied from the center to periphery of irradiated spot (see **Figures 2** and **3**). This dependence was the indicator of that the structure appearance is not in the framework of UPM. After the action of

approximately $N \geq 300$ pulses at the periphery of irradiated zone, the low contrast resonant surface relief with period $d^- = \lambda/(\eta - sin\theta)$ ($\mathbf{g}^-$ || $\mathbf{E}_t$) was observed for <30°. Here θ is the angle of incidence of laser radiation. For >30° the quasi-grating $\mathbf{G}$ disappears, and only the grating $\mathbf{g}^-$ appears at the central part of spot expanding toward periphery frequently in mode of separated tracks which fill much more area with angle θ. Note here that the effective sources of SPP's scattering and incident laser radiation transformation into SPPs are grain boundaries (see, for instance, Ref. [13]).
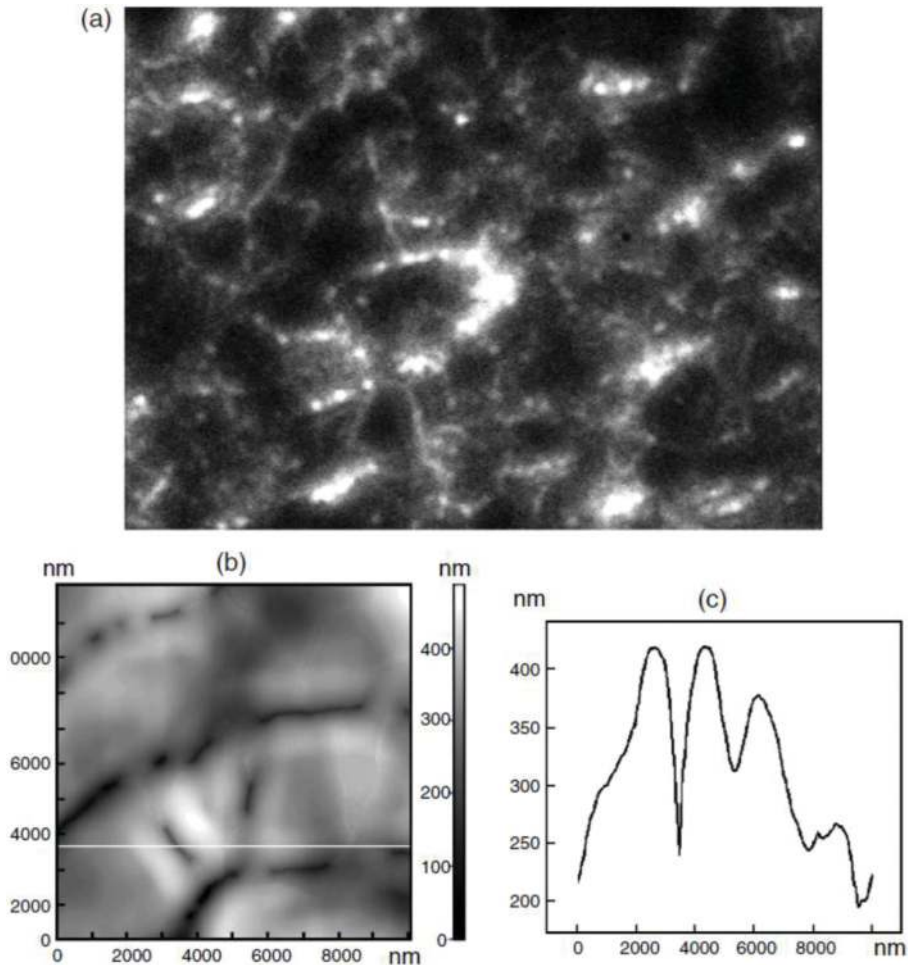

Figure 1. Topography of titanium surface produced under the interaction of 60 pulses of linear polarized laser radiation with power density ≈0.8 MW/cm^2: (a) the initial stage of anisotropic grain growth dark-field optical microtopography, (b) the enlarged view of atomic force topography, and (c) typical profilogram of irradiated surface made along the white line indicated in (b).
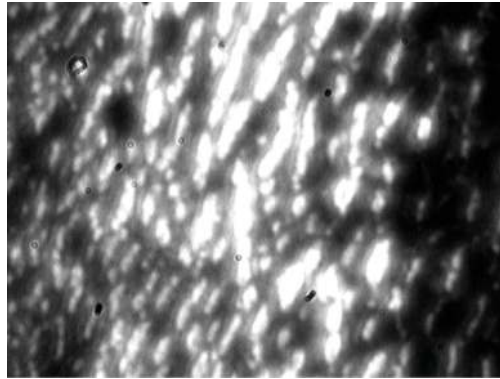
Figure 2. Dark-field optical microscopy image of the titanium surface spot area irradiated by linear polarized laser radiation ($\lambda = 1064$ nm, $\tau = 20$ ns) shows the quasi-grating formation of grooves of thermal grooving.
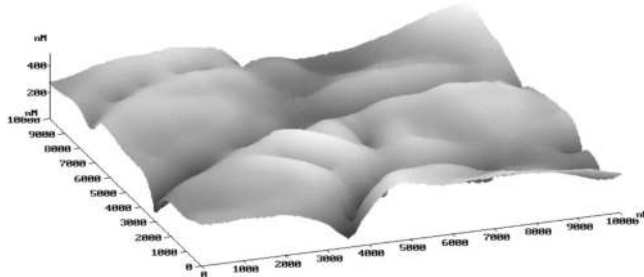

Figure 3. Image of titanium surface irradiated by series of N = 62 pulses of linear polarized laser radiation with $q < q_{melt}$ obtained by atomic force microscopy.

The experiments also were conducted in atmosphere of active and inert gases at atmosphere pressure. The number of laser pulses needed to produce relief of given height in inert gases was higher by $(1.5 \div 2)$ times in comparison with air and was lower by $(2 \div 2.5)$ times in oxygen atmosphere. As is known the formation of resonant gratings by circular polarized laser radiation is difficult because the gratings of all possible orientations (but discrete) must be produced. For this case, the degree of positive feedback via grating height occurs to be insufficient. So, in our experiments for circular polarization, neither resonant gratings nor quasi-grating formation was observed. The experiments were made at laser power density in the range $(0.3 \div 0.8)$ MW/cm^2 to be sure that the melting point of titanium surface will not be achieved.

To study pulse-to-pulse reflectivity dynamics of irradiated area, the integrated sphere and probe radiation ($\lambda = 632.8$ nm) were used. The time dependence of surface absorptivity has shown the shallow minima for $N \approx 40$ followed by gradual rise. The absorptivity change at minima was $\Delta A = A_0 - A_{min} \leq 0.14$, where A_0 is the initial absorptivity value and the A_{min} value

corresponds to surface absorptivity minima; the initial value is $A_0 = 0.5$ (see, for instance, Ref. [14]). In our experiments, the final value of A was near $1.2 A_0$.

The dynamics of surface relief changes was caused by grain boundary displacement in the surface layer of the order of the depth of surface layer pulsed heating. The local minima existence in the function A = A(N) is the consequence of two following process competitions, namely, the collective recrystallization which enhances the optical properties and causes the metal absorptivity falling and oxygen dissolution in metal skin layer and surface oxide film growth cause the absorptivity rising. The experimentally observed evolution of the surface relief on the initial stage is the consequence of technique of its polishing. Really, in the process of mechanical polishing, the metastable highly cold-hardening layer of titanium is formed having properties approaching to ones of amorphous metal. The action of repetitive pulses of laser radiation leads to more equilibrium metal state through the recrystallization process [10]. So in a whole, the process is followed by sufficient grain-size growth of surface layer.

Next discuss the quasi-grating vector **G** orientation correlated with the laser radiation polarization origin. The propagation directions of excited SPPs are mainly along the E_t vector. That is why SPPs most efficiently interact with grain boundaries which have orthogonal to $\mathbf{E}_t$ orientation. The directional SPP's propagation causes the appearance of current of electrons in metal skin layer [15, 16]. The current appears due to the tangential component of the Lorentz force $F_t \sim [v \times H]$ where v is the electron velocity and H is SPP's magnetic field strength vector. The action of the SPP's vertical component of electric field strength vector (E_z) accelerates the skin-layer electrons in vertical direction (v_z) which produces the Lorentz force component along SPP's propagation direction, $\mathbf{F}_t || (k_s/k_s)$. The sign of vertical component of the electric field strength (E_z) is changing simultaneously with the sign of magnetic field strength (H) that is why the direction of the Lorentz force component $\mathbf{F}_t$ always remains along the SPP propagation direction k_s/k_s.

The directed flux of electrons interacts with grain boundaries as with a wall, thus supplying an additional force action and directed grain displacement. Obviously, maximal momentum will transfer to the deformation boundary, which is orthogonal to the SPP's propagation direction. In such a way, the anisotropy of grain growth is rising.
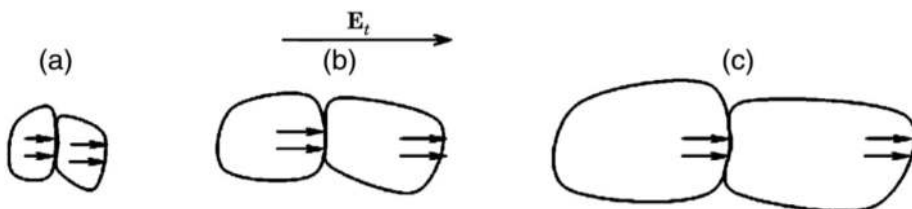

Figure 4. Scheme illustrated the subsequent grain boundary evolution under their interaction with directed flux of skin-layer electrons dragged by laser-excited surface plasmon polaritons. The progressive stages of the grain growth are shown in (a), (b), and (c). The vector orientation of quasi-grating formed at the final stage is $G \perp E_t$.

The process of quasi-grating formation occurs with positive feedback. Qualitatively, the directed flux of electrons action is mostly effective for the grain boundary orientation $n \parallel k_s$, where n is normal to the grain boundary laying in the plane of irradiated surface and k_s is the wave vector of SPP's. Taking in mind the grain boundary continuity, the neighbor boundary areas' curvature reduces. This enhance the efficiency of SPP's excitation (in given direction). This brings about the rise of Lorentz force Ft acting on grain boundaries of neighbor grains for which the direction of normal n is nearly parallel to E_t, (**Figure 4**) This process takes place with the positive feedback and spreads over the irradiated zone. Finally, the self-consistent situation arises in which effective SPP's excitation is realized mainly on almost linear grain boundaries with $n \parallel k_s$. The process is stabilized when SPP's intensity is insufficient to move the grain boundary and their energy is dissipated into the metal. Such situation occurs for the optimal values of typical distances between the neighborhood grooves of formed quasi-gratings of the order of SPP's propagation length $L = 1/\alpha$, where α is the attenuation coefficient of the metal-air boundary for SPPs. The spatial areas of irradiated spot with higher laser radiation intensity are awaited to have the quasi-grating periods higher than for lower power density areas due to nearly linear dependence of excited SPP's intensities on the intensity of incident radiation. This conclusion is supported by our experimental results.

Let us estimate the value of SPP's attenuation coefficient α using the tabulated optical constants for $\lambda = 1064$ nm [14]:

$$\alpha = 2\,\mathrm{Im}k_s = 2k_0\left(\frac{\varepsilon_m}{\varepsilon_m + 1}\right)^{1/2}. \tag{3}$$

Here k_s is the SPP's wave vector's module, ε_m is titanium metal complex dielectric permittivity, $k_0 = \omega/c$ is the wave number of laser radiation in vacuum, ω is the circular frequency of laser radiation, and c is the velocity of light in vacuum. The estimate based on expression (3) and optical constants of titanium for $\lambda = 1064$ nm shows that the SPP's propagation length $L = \alpha^{-1} \approx 4\lambda$ for $\lambda = 1064$ nm and this value well coincides with experimentally measured value $s \approx 5$ μm. For surface areas with higher power density, the s value may reach $(6 \div 6.5)$ μm (see **Figure 2**).

The driving force to displace the grain boundaries is the result of the flux of moving electrons dragged by SPP's interaction with grain boundaries, is limited in depth by titanium skin layer, and is of the order lower than the thermal heating depth. The skin-layer size spatial localization of driving force makes the boundaries displacement process easier. At the final stage of evolution, the **G** quasi-grating relief performs the nearly parallel and equidistant grooves of thermal etching (see **Figures 5a**, **5b**, and **1c**), having the inverse knife structure shapes with the depth up to 500 nm. The cross section of groove has radius of tip curvature of the order 50 nm or less, and dihedral angle at the tip is of the order 120°.
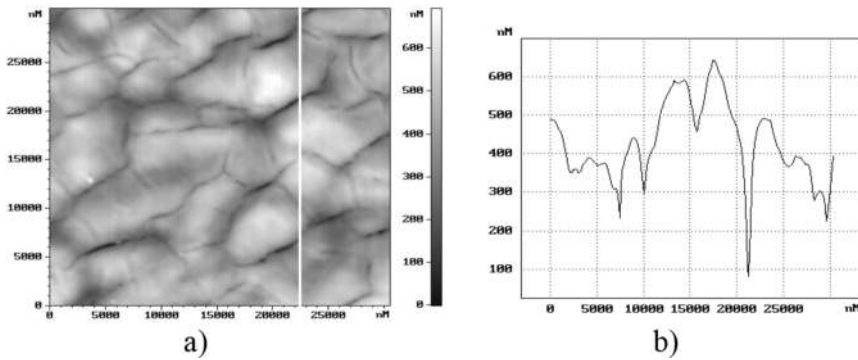
Figure 5. (a) Enlarged fragment of surface area of produced thermal grooves and (b) cross-sectional profile of surface obtained along white horizontal line of **Figure 4a**.

From **Figure 3**, it follows that as a result of multipulsed irradiation, the titanium surface locally becomes sufficiently more smooth than the initial one (surface roughness after surface mechanical polishing, stretching, and so on is smoothing; see **Figure 1b**). This is a well-known result of material redistribution caused by surface atom diffusion [17].

The inverse knife-shaped metal groove can support the channel surface plasmon polariton (CSPP) propagation [3, 5, 18]. In considered geometry of experiment, the direction of quasi-grating vector is orthogonal to laser radiation polarization E_t. For efficient excitation of CSPP, the electric field strength component of incident radiation must be maximal. So, the metal surface covered with quasi-grating has anisotropic absorptivity due to CSPP excitation and dissipation of their energy into heat. It is known that micro- and nanostructured metal surface also has anisotropy of electrical properties [19].

Note that the effect of the electrons drag by surface plasmon polaritons becomes apparent in the surface current in metal skin layer [12, 15] and in the *lateral* flux of relativistic electrons in vacuum under the metal surface irradiation by exawatt laser power density (pulse duration less than 1 ps) [20].

One may wait that the discovered effect may be well observable for powerful ultrashort laser pulse interaction with metals. Really, the experimental data for the multipulsed laser interaction with metals and alloys have been published for femtosecond pulse durations followed by quasi-grating $G \perp E$ formation for titanium metal [21, 22] and Ti-based alloy Ti-Zr-Cu-Pd [23] without any suggestions about the origin of their appearance (see **Figure 6**). From our opinion the production mechanism of quasi-grating G superimposed on the $g \parallel E$ resonant grating is analogous for one suggested for nanosecond irradiation regime. Note that the thermal etching groove formation is inherent to (poly)crystalline materials, but the alloy Ti-Zr-Cu-Pd is the amorphous one. In fact under the alloy heating up to high temperature, the alloy transfers from its metastable state to the crystalline one, and the suggested model works further.
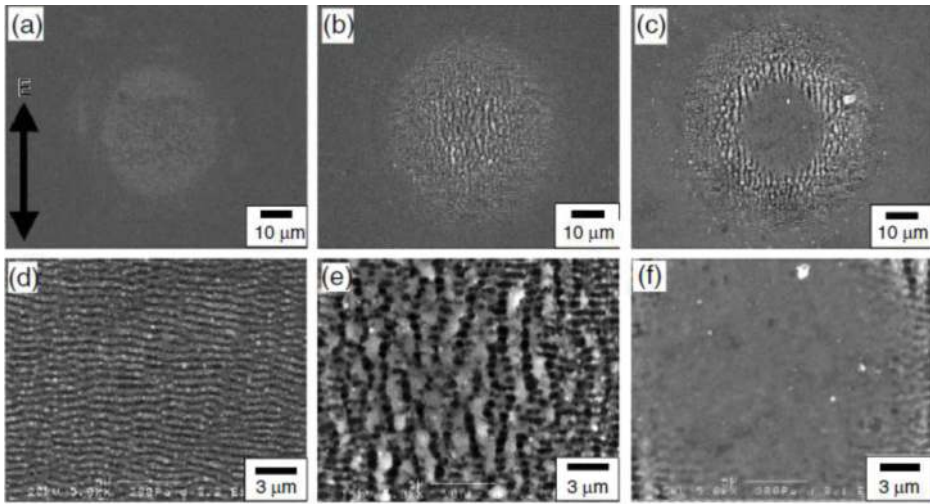
Figure 6. The quasi-periodic microrelief obtained on a titanium surface under the action of ultrashort pulses (τ = 150 fs, λ = 800 nm, pulse-repetition rate 1 kHz, N =10) for energy densities Q = 0.25 J/cm^2 (a) and (d), 0.75 J/cm^2 (b) and (e), and 1.5 J/cm^2 (c) and (f) at low (upper row) and high magnification (lower row), $\mathbf{g} \perp \mathbf{E}_t$ [21].

In one of the previous models proposed for explanation of spatial periodic relief on metal surfaces under ultrashort laser illumination [24], the process was considered with nucleation in a distended metal and the ensemble of cavitating bubble self-ordering [24]. According to authors [24] and physics of the process, the orientation and periods of produced nanostructures are independent on laser radiation polarization and wavelength, accordingly. The typical power densities of laser radiation must be higher than in our consideration. In this model, the predicted spatial periods are of the laser heating depth (10 ÷ 100) nm order. Hence, the model [24] is not applicable for our case.

3. Effect of electroplasticity

The effect of electroplasticity will be considered in this section as one of the most closed volume analog for anisotropic grain boundary movement (AGM) effect (Section 2). At first the electroplasticity effect (EPE) in metals was discovered by Troitsky [25]. The metals demonstrate the enhanced plasticity under the influence of the high directed current density.

The high perfection of axial texture is formed due to metal grains of definite crystallographic orientations turned in the direction of wire dragging (**Figure 7**). The initial material takes the texture "suitable" for subsequent high current transfer [26]. This structure turns out more perfect than that formed by the usual wire-dragging technology. During electro-plastic wire dragging, the deformation strengthening fails and the plasticity increases as a result [27–35].
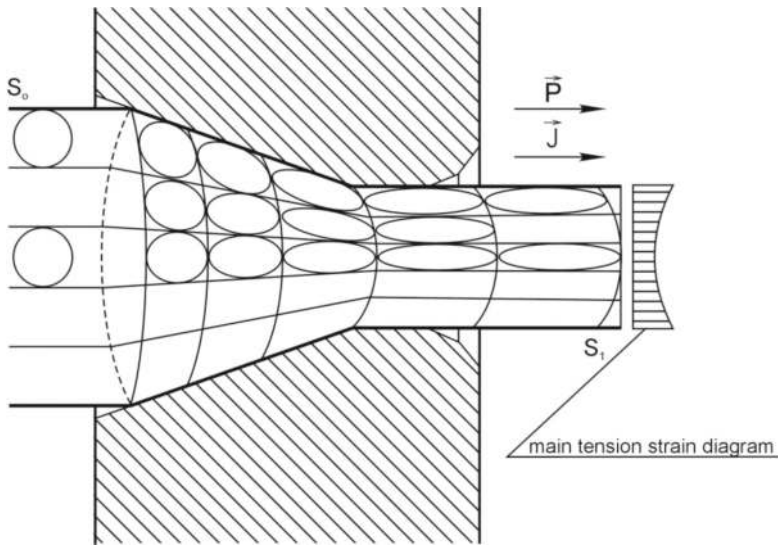
Figure 7. The perfect wire texture creation during electro-plastic wire dragging in condition of current density **j** and wire movement direction **P** vector coexistence [26].

The thorough analysis shows that the nonthermal current action mechanisms involve electro-plastic effect and ponderomotive forces of pulsed current and impact the wire tension decrease sufficiently. More efficient pulsed current action (in comparison with dc) [26, 30], current polarity dependence evidence the nonthermal nature of the occurred processes. In addition, during rapid wire dragging (>10 m/s), the Stewart-Tolman effect takes place (the delay of free electron gas against crystal lattice accelerating in the area of metal deformation inside a drawing ring caused by transition to a smaller diameter). The Stewart-Tolman effect is electronic by nature, and it favors the axial wire texturing to the electro-plastic and its degree of perfection increasing. The typical parameters realized under the electro-plastic effect are listed below:

- Frequency of current flow (10 kHz)

- Current power density (250 kA/cm^2)

- Current pulse duration (60 μs)

- Wire-dragging velocity (rapid dragging) (≥10 m/s)

The observed effect is caused by plasticity influence of EPE in metal volume; it relieves the process of axial texture formation and decreases friction in dragging die due to the grain crush in the near-surface wire areas.

Apart from the perfect grain structure creation for copper, it was observed as follows [26]:

- The number of randomly distributed dislocations decreases.

- Wire electrical resistivity decreases by 8–15%.

- Wire residual plasticity increases by 25–30%.

- Wire-dragging force decreases by 25–30%.

For the stainless steel wire, it was observed as follows [26]:

- Electrical resistance decreases by 18–20% in comparison with warm wire dragging and by 26–30% in comparison with cold wire dragging without current.

- Residual plasticity increases by 5–20%.

- The strength limit decreases by 15–20%.

The electroplasticity effect is a linear function of current density and was never observed for alternated current. It is known that to remove inner tension and residual deformations on high-voltage transmission equipment, the powerful pulse current is transmitted by the wires hanged preliminary before the wires are to be arranged finally.

So, in general, the electroplasticity effect may be considered as a volume analog of the effect of anisotropic grain boundary movement (AGM) being discussed. Really, the electroplasticity effect is caused by directed current of electrons' action. And the AGM effect is also the consequence of the direct current of electrons forced by the effect of electrons drag by surface plasmon polaritons in optical skin layer of metal. In both cases, the directed electrons transfer their momentums to the grain boundary as a wall and force their displacement.

4. Conclusion

The formation of microstructures on metal surface under the interaction of laser radiation of nanosecond durations in regime of near-threshold melting was theoretically and experimentally analyzed. The generations of regular structures in mode of linear gratings or normal and abnormal orientations the periods of which are proportional to laser radiation wavelength were observed. The mechanisms of discussed structure formation are in frameworks of universal polariton model of laser-induced condensed mater damage. In the regime of power density not exceeding the melting threshold, the relief of a new type in mode of quasi-grating of grooves with periods of the order 5 μm and grating orientation orthogonal to the electric field strength vector of laser radiation has been studied. So, the anisotropy of grain growth process was observed. To explain the result of anisotropic growth, the qualitative model was suggested. The model is based on the effect of skin-layer electrons dragged by surface plasmon polaritons. The flux of electrons transfers its momentum to the grain boundary as to the wall given an anisotropic force. So, the produced skin-depth surface layer has properties differing from the bulk of metal.

The considered effect is the surface one. As the volume analog to this effect the well-known electroplasticity, one can be considered. Really, in both cases, the cause of the main effect in metal is the directed flux of electrons.

Author details

Makin Vladimir Sergeevich

Address all correspondence to: makin@sbor.net

Scientific Research Institute for Opto-Electronic Device Instrumentation, Sosnovy Bor City, Leningrad Oblast, Russia

References

[1] Bonch-Bruevich A.M., Libenson M.N., Makin V.S., Trubaev V.V. Surface electromagnetic waves in optics. Opt. Eng. V. 31. No. 4. Pp. 718–730 (1992).

[2] Makin V.S., Makin R.S. Nonlinear interaction of linear polarized laser radiation with condensed media and overcoming the diffraction limit. Opt. Spectrosc. V. 115. No. 2. Pp. 162–167 (2012).

[3] Makin V.S., Pestov Y.I., Makin R.S. Abnormal spatial nanogratings formation by long pulse laser radiation on condensed matter surfaces. Proceedings of International Conference "Days on Diffraction". 2016. Pp.298–303.

[4] Makin V.S., Logacheva E.I., Makin R.S. Origin of anomalous nanostructures formation under linear polarized femtosecond laser irradiation of condensed matter. Proceedings of International Conference "Days on Diffraction". 2015. Pp. 201–207.

[5] Makin V.S., Logacheva E.I., Makin R.S. Localized surface plasmon polaritons and nonlinear overcoming of the diffraction optical limit. Opt. Spectrosc. V. 120. No. 4. Pp. 610–614 (2016).

[6] Makin V.S., Makin R.S. Interaction of laser radiation with an axially symmetric polarization with condensed media. Opt. Spectrosc. V. 115. No. 4. Pp. 591–595 (2013).

[7] Olemskoĭ A.I. Synergetic of complex systems. Moscow. Kasandr. 2009.

[8] Schmidt S., Nielson S.F., Gundlach C., Margulies L., Huang X., Juul J.D. Watching the growth of bulk grains during recrystallization of deformed metals. Science. V. 305. P. 229 (2004).

[9] Han-Riege C.S., Thompson C.V. Microstructural evolution induced by scanned laser annealing in Al interconnects. Appl. Phys. Lett. V. 75. P. 1464 (1999).

[10] Gulyaev A.P. Physical metallurgy. Moscow. Mashinostroenie. 1986.

[11] Makin V.S., Makin R.S., Vorobiev A.Y., Guo C. Feigenbaum's universality and Sharkovsky order in laser-induced periodical structures at interfaces and in bulk of

condensed matter. In Nonlinearity in modern nature. Editor Malinetskii G.G. Moscow. LKI Publisher. 2009. Pp. 303–322 (in Russian).

[12] Libenson M.N., Bonch-Bruevich A.M., Makin V.S. Surface polaritons and powerful radiation action. Usp. Fiz. Nauk. V. 155. P. 719 (1988) [Sov. Phys. Usp. 31, 772 (1988)].

[13] Samblse J.R. Grain-boundary scattering and surface-plasmon attenuation in noble-metal films. Solid State Commun. V. 49. P. 343 (1984).

[14] Johnson P.B., Christy R.W. Optical constants of the transition metals: Ti, V, Cr, Mn, Fe, Ni, and Pd. Phys. Rev. B. V. 9. P. 5056 (1974).

[15] Mikheev G.M., Nasibulin A.G. Photon drag effect in single-walled carbon nanotube films. Nano Lett. V. 12. No. 1. Pp. 77–83 (2012).

[16] Durach M., Rusina A., Stockman M.I. Giant surface-plasmon-induced drag effect in metal nanowires. Phys. Rev. Lett. V. 103. P. 186801 (2009).

[17] Geguzin Y.E., Ovcharenko N.N. Surface energy and surface processes in solids. Usp. Fiz. Nauk. V. 76. P. 283 (1962) [Sov. Phys. Usp. 5, 129 (1962)].

[18] Bozhevolnyi S.I., Volkov I.S., Devaux E., Laluet J.-K., Ebbesen T.W. Channel plasmon polariton guided by subwavelength metal grooves. Phys. Rev. Lett. V. 95. P. 046802 (2005).

[19] Chiappe D., Toma A., de Mongeo F.B. Tailoring resistivity anisotropy of nanorippled metal films: electron surfing on gold waves. Phys. Rev. B. V. 86. P. 045414 (2012).

[20] Makin V.S., Makin R.S. Lateral relativistic electron beam synergetic creation and transport by petawatt laser radiation. Proceedings of International Conference Days on Diffraction, May 30–June 3, 2011, St-Petersburg, Russia. Pp. 133–136.

[21] Tsukamoto M., Asuka K., Nakano H., Hashida M., Katto M., Abe N., Fujita M. Periodic microstructures produced by femtosecond laser irradiation on titanium plate. Vacuum. V. 80. P. 1346 (2006).

[22] Vorobyev A.Y., Guo C.L. Femtosecond laser structuring of titanium implants. Appl. Surf. Sci. V. 253. P. 7272 (2007).

[23] Shinonaga T., Tsukamoto M., Mariyama S., Matsushita N., Wada T., Wang X., Honda H., Fujita M., Abe N. Femtosecond and nanosecond laser irradiation for microstructure formation on bulk metallic glass. Trans. JWRI. V. 38. No. 1. P. 81 (2009).

[24] Zhakhovskiĭ V.V., Inogamov N.A., Nishihara K. New mechanism of the formation of the nanorelief on a surface irradiated by a femtosecond laser pulse. Pis'ma Zh. Eksp. Teor. Fiz. V. 87. P. 491 (2008) [JETP Lett. 87, 423 (2008)].

[25] Troitsky O.A. Electromechanical effect in metals. Pis'ma v JETF. V. 10. P. 18 (1969).

[26] Troitsky O.A., Stashenko V.I., Ryszkov V.G., Lyashenko V.P., Kobyl'skaya E.B. Electro-plastic wire-dragging and new technologies to simplify wire creation. Problems of

Atomic Science and Techniques. Seria: Physics of Radiative Damage and Radiative Material Science. V. 4. No. 98. Pp. 111–117 (2011).

[27] Gromov V.E., Zuev L.B., Kozlov E.V., Tsezermayer V.Y. Electrostimulated plasticity of metals and alloys. Moscow. Nedra. 1996. 280 p.

[28] Roschupkin A.N., Troitsky O.A., Spitsin V.I., et al. The high density current action on metal plastic deformation conception development. Dokl. AN SSSR. V. 286. No. 3. Pp. 633–636 (1986).

[29] Mel'nikova N.V., Hon Y.A. To the theory of electroplastic deformation of metals. Phys. Mesomech. V. 3. No. 5. Pp. 59–64 (2000).

[30] Dubinko V.I., Kras V.I., Klepikov V.F., Ostapchuk P.N., Potapenko I.F. Enhanced Plasticity under the electric current pulses action modeling. Problems of Atomic Science and Technique. Series: Physics of Radiative Damage and Radiative Material Science. V. 2. No.4 Pp.158–166 (2009).

[31] Kravchenko V.V. Directed electron's flux action on moving dislocations. JETF. V. 51. Pp. 1676–1681 (1966).

[32] Malygin G.A. Self-organization dislocations process and plasticity of crystals. Usp. Fiz. Nauk. V. 169. No. 9. Pp. 979–1008 (1999).

[33] Spitsin V.I., Troitsky O.A., Ryzhov V.G., Kozyrev A.S. On-draw-plate copper wires dragging. Dokl. AN SSSR. V. 231. No. 2. Pp. 402–404 (1976).

[34] Spitsin V.I., Troitsky O.A. Electro-plastic deformation of metals. Moscow. Nauka. 1985. 160 p.

[35] Troitsky O.A. Ultrasound electroplastic flatting of metals. Bulletin for Science-Technology Development. National Technology Group. V. 10. No. 26. Pp. 42–49 (2009).